Journal of Structural Geology, Vol. 7, No. 5, pp. 541 to 553, 1985
Printed in Great Britain

0191-8141/85 $03.00 + 0.00

Cathodoluminescence petrography of syntectonic quartz fibres

DOROTHEE DIETRICH

Geologisches Institut, ETH Zentrum, CH-8092 Zürich, Switzerland

and

PAUL R. GRANT

Department of Geology, Royal School of Mines, Imperial College, London SW7 2BP, U.K.

(*Received* 9 *February* 1984; *accepted in revised form* 14 *November* 1984)

Abstract—The cathodoluminescence of low grade metamorphic quartz is reported in the literature to be uniformly brown. This study describes an investigation of syntectonic quartz fibres from veins and pressure shadows contained in different carbonate units of the Helvetic Alps, Switzerland, and of Anglesey, U.K., with the Scanning Electron Microscope in the cathodoluminescence mode. The cathodoluminescence spectra measured show systematic variations between older and younger parts of the same fibre, and between fibres from different tectonic units. These variations can be related first to variations in the temperature of formation of the quartz fibres, and second to deformation-induced differences in the microstructure of the earlier formed parts of fibres during later imposed strains.

INTRODUCTION

WHEN a material is bombarded by electrons, the specimen-beam interactions cause electromagnetic radiation from the sample. The visible range of this electromagnetic spectrum, with slight excursions into the near ultraviolet and near infrared, is termed cathodoluminescence (CL). Geologists normally encounter CL through microprobe studies or on specialised CL-attachments to optical microscopes. Any beam of electrons has the potential to generate CL provided certain minimum limits of current flux and electron energy are exceeded in the beam (Muir & Grant 1974).

Cathodoluminescence potential is high for distinguishing optically subtle differences in species of minerals, or variations in one species due to changing chemical and/or physical conditions during growth, or post-crystallization modifications of crystal lattices. Geological examples of these are respectively:

(1) the orthorhombic and the trigonal carbonates show different luminescence spectra. There is a systematic shift of the peak of the luminescence related to different gross symmetry and cation radius (Sommer 1972);
(2) diamond, cassiterite, carbonates and so on display growth zoning if viewed under CL which may not be apparent optically and
(3) carbonates and quartz exhibit 'strain contrast' at point contacts between grains that have been compressed (U. Zinkernagel, pers. com.).

Cathodoluminescence may be a sensitive indicator of any strain present in a crystal because the energies involved in the electron bond transitions in the CL range are relatively low. Also, lattice disturbances due to variations in dislocation density or style, or to point defect density, distribution or occupancy may cause different CL properties (Holt & Odgen 1976).

In this study we investigate syntectonically grown quartz fibres from different localities, which can be related to different deformation histories of the adjacent rock matrix.

Quartz displays gross variations in luminescence colour and intragranular texture that are related to provenance, diagenetic alteration and metamorphic alteration (Grant & White 1978, Sibley 1975, Sprunt 1981, Zinkernagel 1978). Thus, high grade metamorphic quartz can be distinguished from diagenetic quartz by virtue of CL colour and texture. High grade metamorphic quartz usually luminesces bright blue and, if the grains are highly deformed (e.g. quartz from gneisses), they show a dark criss-cross network (Sprunt *et al.* 1978). Diagenetic quartz overgrowths are very weakly luminescent. However, with a highly efficient detector, patterns reflecting crypto- or microcryst development of the overgrowth can be distinguished (Grant & White 1978). Contact metamorphosed quartz usually shows the same CL colour as deformed and high grade regionally metamorphosed quartz, but not the criss-cross pattern. More subtle differentiations are also possible. For example, quartz derived from volcanic sources often displays a core and mantle structure when viewed under CL (Zinkernagel 1978) especially if there are also resorbtion features around the rims of the grains.

Low grade metamorphic quartz, which includes all the fibres studied here, has up to now been found to be uniform in colour and to show little textural variation. This work represents therefore a test of the discriminatory potential of the CL method when applied to geneti-

cally fairly homogeneous quartz. All the fibres studied consist of quartz derived from pressure solution of quartz clasts present in carbonate rocks and subsequently redeposited in fibrous form during the deformation of the limestones. In the following we characterize the CL spectra of the different fibre types and we relate the CL properties to the fibre growth history.

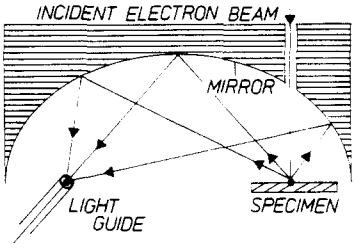

Fig. 1. Cross section through an ellipsoidal CL detector showing the CL ray paths.

METHOD OF CATHODOLUMINESCENCE MEASUREMENT

The specimens were standard microprobe polished thin sections with a light carbon coat (~500 Å). The Scanning Electron Microscope (SEM) used was a JEOL JSM 35. In all cases, except when specified, a working voltage of 30 kV was employed. The beam current could not be monitored but was kept as near constant as possible during specific runs.

The cathodoluminescence detector

A semiellipsoidal mirror with light guide and spectrometer was used to collect and analyse the CL (Steyn *et al.* 1976). The semiellipsoidal mirror takes advantage of the fact that linear rays passing through one focus of the ellipsoid will be reflected back through the second focus. Hence a semiellipsoidal mirror is arranged to have one focus centred on the electron optical column (Fig. 1). The specimen can be moved below the mirror so that regions of interest can be brought to this focus. At the second focus is a lens and a light guide which collects the light and transmits it out of the SEM to the spectrometer. The spectrometer may be arranged so that all the incident light is 'seen' by a photomultiplier and the signal fed back into the SEM monitoring screen to produce a panchromatic CL map of the specimen. Alternatively the spectrometer can be scanned and the signal from the light-collecting photomultiplier fed into a simultaneously scanning multichannel scaler. This produces a histogram-type plot of the intensity of CL against wavelength. These raw data, though instructive, do not give a true interpretation of the actual intensity of the emitted luminescence. The collected data are distorted by nonuniform responses of the light guide, spectrometer and, dominantly, the photomultiplier. If absolute emission intensities are required, a correction has to be applied. This correction is different for different wavebands, but generally for about 400 nm it is a minimum and increases monotonically in either direction. For a further discussion of the technicalities of the method and a comparison of SEM CL vs optical CL see Holt & Odgen (1976) and Grant (1978).

The spectra measured for this study were obtained in various runs, the results of which are not always comparable. Although the intensities (photon count sec^{-1}) of individual peaks of different spectra are not comparable, the proportions of each component wavelength are constant. A quantitative description of the spectra can be obtained in a simple way. Assuming that the curves which characterize the peaks are Gaussian, the product of height times half-width of a peak can be considered a measure of its relative intensity. For a comparison of different spectra we used the intensity ratio of the two peaks contained in most of our spectra.

Advantages and disadvantages of SEM cathodoluminescence

The advantage of this method for a comparative study is that the CL of a point in a scanned specimen can be registered graphically as a spectrum and can therefore be compared easily with other CL measurements from the same or from different specimens. On the other hand, SEM CL images can be difficult to obtain, as pointed out by Grant (1978). Theoretically, the spatial resolution of diffraction should be limited by the optical optimum, but practically this does not seem to be so. Only luminescence with rapid response times can be successfully observed in the SEM. Although 'phosphoresecing' materials cause insurmountable problems for imaging, spectra can be successfully obtained. SEM CL images are the final visual representation of intermediate electronic signals. These signals can be amplified and manipulated in ways not available with CL-attachments to optical microscopes.

CATHODOLUMINESCENCE OF QUARTZ FIBRES

Pressure shadows

Pressure shadows around pyrite crystals are a common feature in the Helvetic nappes. They consist of fibrous quartz, but sometimes also of calcite and chlorite. The fibre geometry can be used to describe the sequence of progressive deformation of the nearby rock matrix (Durney 1971, Durney & Ramsay 1973). A recent investigation of the texture of the Helvetic limestones of western Switzerland by Dietrich & Song (1984) has shown that in the area of high deformation, which is indicated by pressure shadows and other strain markers, there exist two regionally distinct textural patterns: (1) a characteristic preferred orientation of the calcite *c*-axes localized along the root zone of the Helvetic nappes and (2) a random pattern present in the Fernigen syncline, in which Helvetic sediments are infolded in the Aar massif. It has been proposed by Dietrich & Song (1984) that two

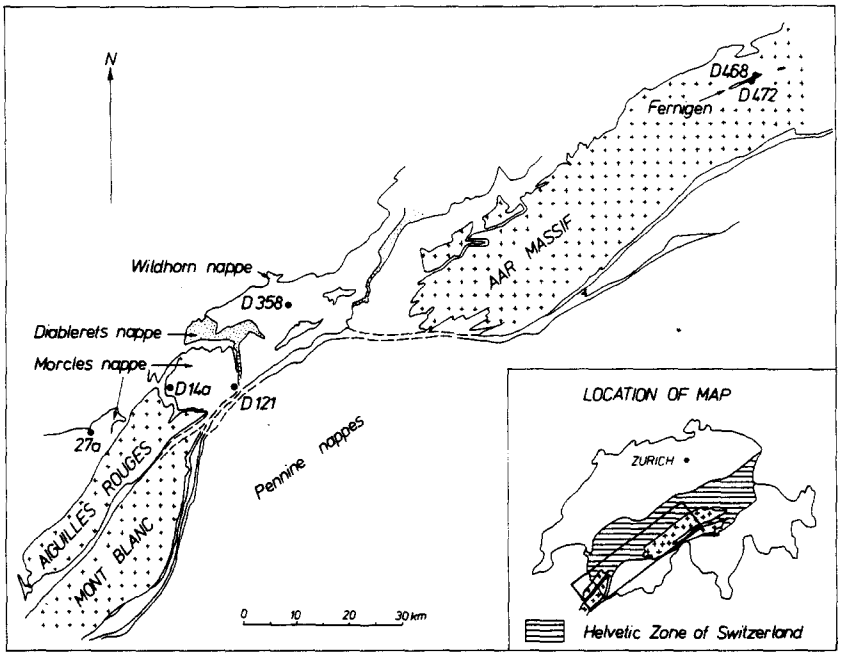

Fig. 2. Tectonic sketch map of the Helvetic nappes of western Switzerland, with specimen localities.

different deformation mechanisms are associated with these patterns: strain-induced recrystallization in regions where preferred orientation occurs, and an intercrystalline deformation mechanism such as grain boundary sliding in regions where random texture patterns exist. The smaller grain size of the Fernigen limestones would tend also to favour intercrystalline mechanisms.

CL spectra were measured from pressure shadow fibres of both areas, and it was found that significant differences in these spectra could be related to the different deformation mechanisms proposed for the limestone matrix. Figure 2 is a tectonic sketch map with the specimen localities.

Specimen D 121 comes from the root zone of the Morcles nappe at Ardon where a good calcite preferred orientation has been found (Fig. 3). The fibres consist of quartz and indicate two successive sub-perpendicular extension directions of the rock matrix. The growth sense of the fibres is antitaxial, that is, towards the pyrite, the criteria for growth sense being the increasing widening of the fibres in the growth direction as well as the increasing degree of preferred orientation of their quartz *c*-axes towards the pyrite (Durney & Ramsay 1973). The longer part of the pressure shadow, with approximately N–S trending fibres, would therefore be older than the shorter part, with E–W trending fibres. We measured consistently similar CL spectra from 11 points on the older part of the pressure shadow. From 13 points on the younger part of the pressure shadow we measured spectra that were consistently similar, but different from those obtained from the older part. CL spectra derived from the two parts are shown in Fig. 4. Both spectra have a red band at about 600 nm. However, the spectrum representative of the older part of the pressure shadow (Fig. 4a) has a markedly better developed blue band at 400 nm than the spectrum for the younger fibres (Fig. 4b), which shows only a subsidiary blue shoulder. We can postulate that there exists a decrease in the proportion of the blue spectral component from the older part of the fibres towards the younger part. This is also seen in the intensity ratios given in Table 1.

Specimens D 468 and D 472 come from the Fernigen syncline, where no preferred orientation of calcite has

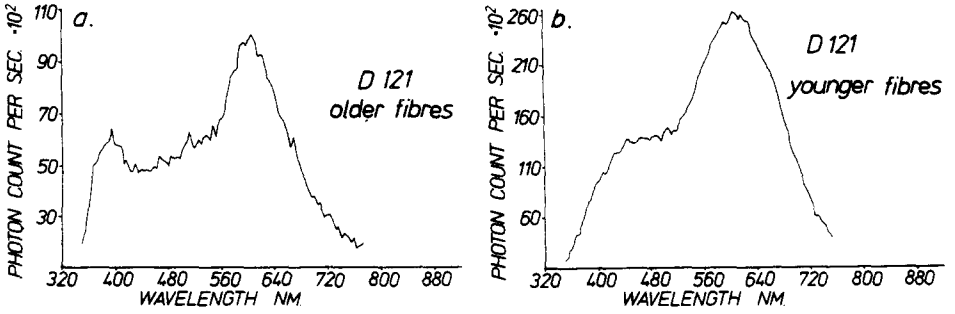

Fig. 4. Spectra from the pressure shadow of D 121. (a) Spectrum from the older part of the fibres. (b) Spectrum from the younger part of the fibres.

been found in the rock matrix (Figs. 2 and 5). The fibres consist of quartz and indicate only one main extension direction in the surrounding limestone. They are thicker than those found in pressure shadow fibres from the Helvetic root zone (Fig. 3). The fibres grew perpendicular to the pyrite wall, the growth sense again being antitaxial. This kind of wall-controlled fibre growth has been related by Durney & Ramsay (1973) to crystal growth on the walls of euhedral pyrite, as is evident in specimen D 468. Specimen D 472 consists of framboidal pyrite and thin, partly recrystallized fibres on the upper side, euhedral pyrite and with thick fibres on the lower side. The fibre geometry can be related to the control which the pyrite morphology exerts on fibre growth. We measured CL from 17 points of D 468, and from 6 points of D 472, but could find no significant differences. The spectra recorded along an individual fibre do not vary in the thicker or thinner fibres, nor in different parts of the measured pressure shadows. Figure 6 shows a spectrum which is therefore indicative of all the measurements taken from the two Fernigen specimens. If we compare the relative intensities of the red and the blue peaks in the spectra of specimen D 121 with the relative intensities of the two peaks in the spectra of specimens D 468 and D 472, the blue band appears to be more weakly developed in the spectra of the Fernigen specimens. This results in a narrower and relatively more pronounced red band in the Fernigen quartz fibre spectra. A clear shift towards red in the red/blue intensity ratios listed in Table 1 can therefore be seen in these spectra.

In interpreting the spectra from the two areas it is necessary to point out that there exists a relation between the development of the two colour bands in quartz and its degree of 'crystallinity'. Quartz of a well-ordered lattice structure luminesces with a strong single blue band, whereas diagenetic quartz luminesces red and typically produces a broad band/low intensity spectrum without a defined blue peak. The blue band has been suggested to be due to very weak O–O π bonds (Hanusiak & White 1975). This has been confirmed by new observations made at low temperatures on natural quartz crystallized at different temperatures. (The crystallization temperatures have been determined by unpublished fluid inclusion studies of P. Alman-Ward & A. Rankin). The results of these CL observations indicate that the blue luminescence has an inverse dependency on the temperature of observation to about −268°C; below −110°C there was little significant increase in luminous yield because the electronic states had become as tightly constrained as possible. We also found that two samples, which crystallized at different temperatures but were examined under identical conditions, reached the same maximum intensity below

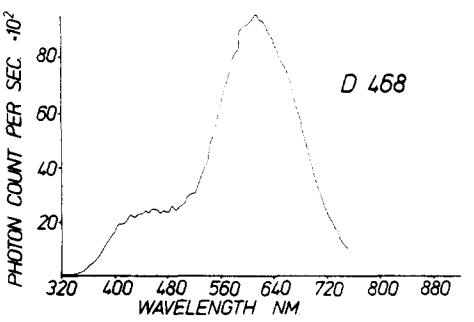

Fig. 6. Spectrum for the pressure shadows of specimen D 468.

Table 1. The intensity ratios (red peak/blue peak) of the spectra measured at 30 kV. The relative intensities for each peak were calculated as height times half-width of the peak. In the case of 'blue shoulders', where no clear peak is developed, the measurement was taken at 400 nm

Specimen		Spectrum in Fig. No.	Peak	Relative intensity $a \cdot b$	$\frac{a \cdot b \text{ of red peak}}{a \cdot b \text{ of blue peak}}$
D 121	Helvetic root zone, older fibres	4a	blue red	3.78 12.15	3.21
D 121	Helvetic root zone, younger fibres	4b	blue red	1.6 16.63	10.39
D 468	Fernigen	6	blue red	0.65 12.68	19.51
	Anglesey, older fibres	10a	blue red	7.38 19.44	2.63
	Anglesey, younger fibres	10b	blue red	1.6 12.16	7.6
D 358	Wildhorn nappe	11	blue red	8.58 17.01	1.98
D 14a	Morcles nappe, older part of vein fibres	13a	blue red	4.0 9.88	2.47
D 14a	Morcles nappe, younger part of vein fibres	13b	blue red	2.4 14.43	6.01
D 14a	Morcles nappe, blocky part of vein	13c	blue red	0.7 12.26	18.94
27a	Morcles nappe, clast	15a	blue red	5.16 3.79	0.73
27a	Morcles nappe, crack–seal vein	15b	blue red	4.68 13.8	2.95

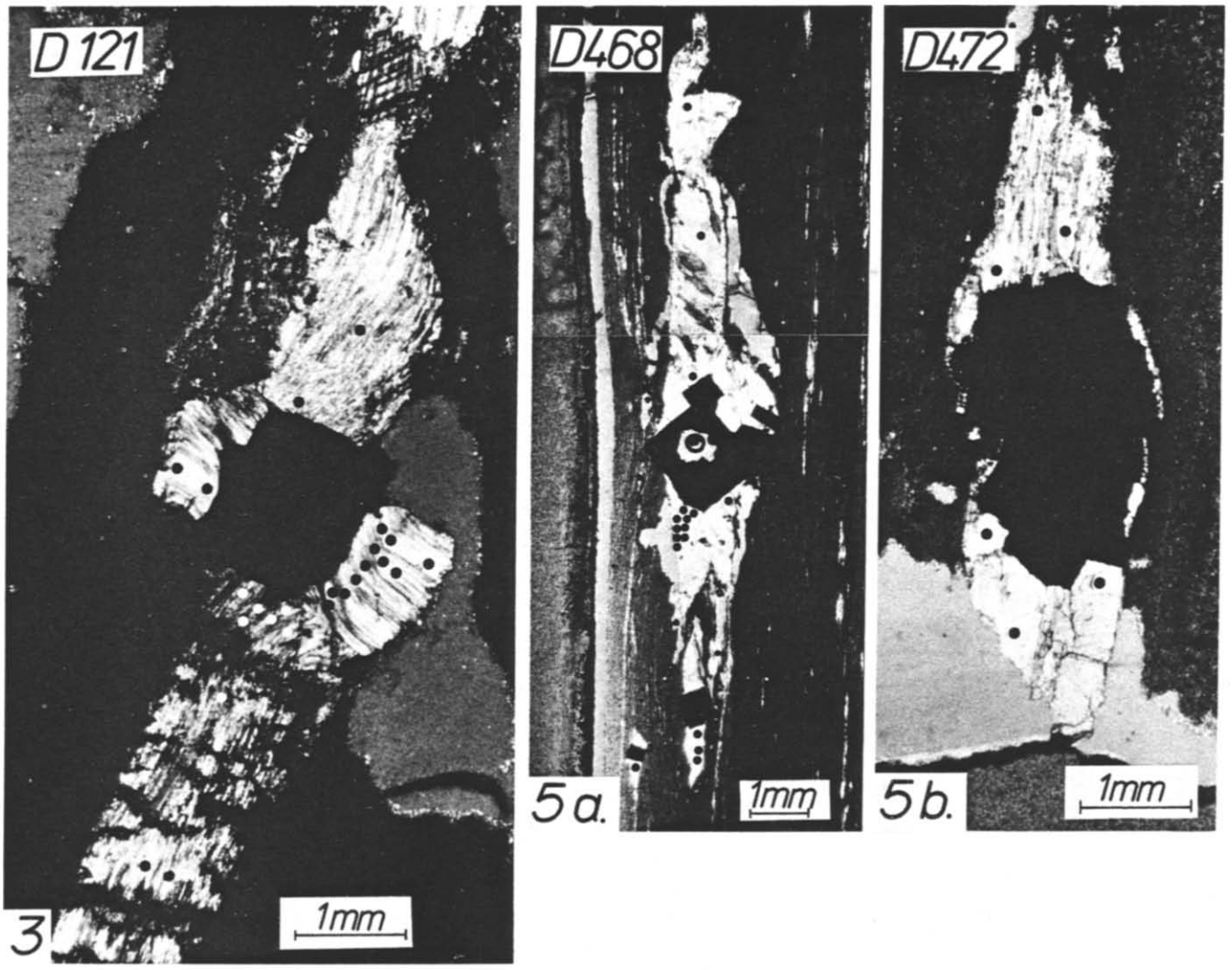

Fig. 3. Pressure shadow with quartz fibres around pyrite; Specimen D121. Micrograph parallel to the cleavage plane, that is the *XY*-plane of the finite strain ellipsoid. The points indicate locations of CL measurements.

Fig. 5. Pressure shadows with quartz fibres around pyrites. (a) Specimen D 468. Micrograph perpendicular to the cleavage plane and parallel to the stretching lineation. (b) Specimen D 472. Micrograph parallel to the cleavage plane.

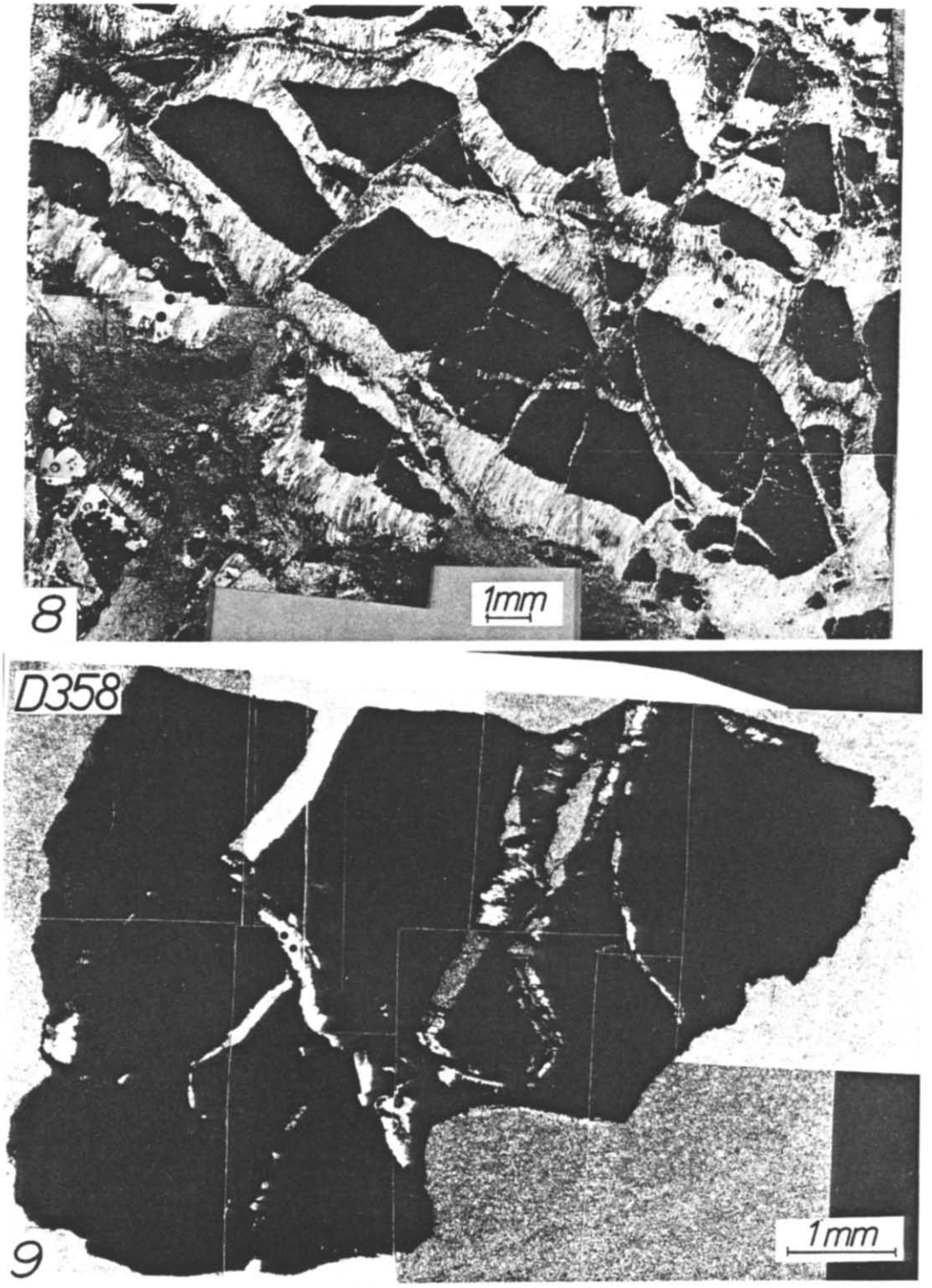

Fig. 8. Chocolate tablet structure from Parys Mountain, Anglesey, with quartz fibres between pyrite plates. The points indicate locations of CL measurements. (Specimen from J. G. Ramsay.)

Fig. 9. Chocolate tablet structure from the Wildhorn nappe (specimen D 358). The points indicate locations of CL measurements.

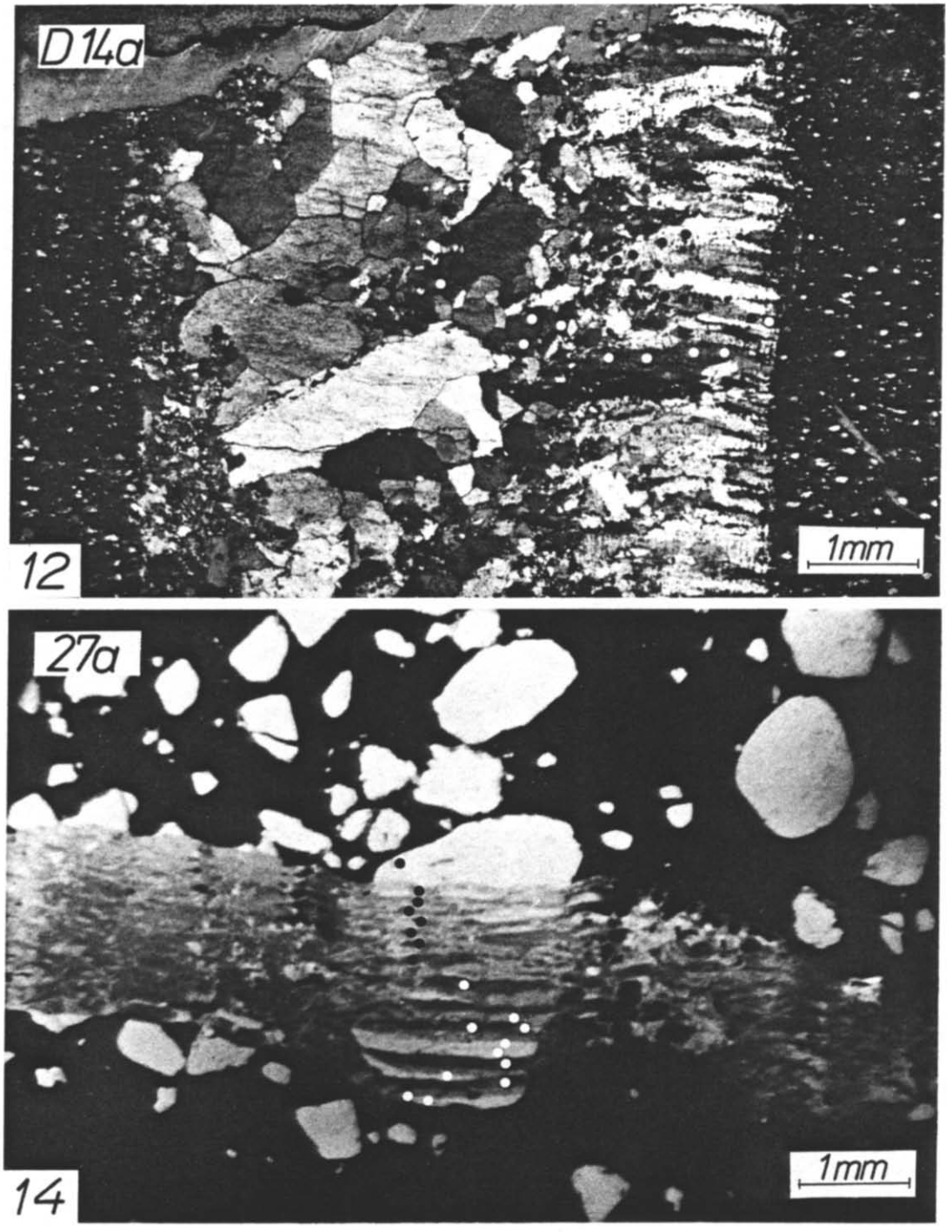

Fig. 12. Vein with antitaxial crack–seal fibres (right side) and blocky crystals (left side) (specimen D 14a). The points indicate locations for CL measurements.

Fig. 14. Optical CL micrograph of crack–seal vein (specimen 27a). Pre-Alpine quartz clasts luminesce violet, Alpine vein quartz luminesces blue. Micrograph was taken by U. Zinkernagel at operating voltage of 5 kV. Points indicate locations for part of the SEM–CL measurements.

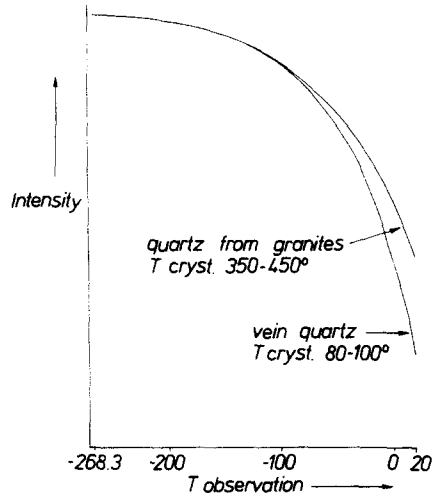

Fig. 7. Two examples of the variation of intensity of the blue band with temperature of observation, normalized at −268.3°C. Temperatures of crystallization were determined using fluid inclusions. (Specimens are from P. Alman-Ward & A. Rankin.)

−110°C (Fig. 7). This indicates that the maximum intensity reflects the beam penetration and excitation volume within the quartz, and not the original quartz microstructure. The blue excitation can therefore be assumed to be directly related to the silica tetrahedra, in agreement with the conclusions of Hanusiak & White (1975). In contrast, the intensity of the red band seems to be much less strongly affected by the temperature of observation. The overall CL colour spectrum of quartz, however, does depend upon the original crystallization temperature and upon the proportion of the blue and red spectral components. There appears to be a critical crystallization temperature which controls the CL colour: quartz crystallized below 150°C luminesces red, whereas quartz crystallized above 150°C luminesces blue.

The different deformation mechanisms inferred for the Helvetic root zone and the Fernigen limestones can be related either to an increase in temperature or to a decrease in strain rate or stress from the root zone towards Fernigen (see for example the deformation mechanism map of Schmid 1982). Illite crystallinity data from both regions show a comparable range of values. We found Kübler indices (Kübler 1968) for the Helvetic root zone varying from 3.4 to 5.5, and Frey *et al.* (1980) found values for the sedimentary cover of the Aar massif varying from 3.7 to 5.1. Consequently we conclude that the Fernigen limestones were deformed under a lower differential stress or at a lower strain rate than the limestones of the root zone. We think that this is expressed in the characteristic shape of the Fernigen quartz fibre spectra.

Chocolate tablet structures

The chocolate tablet structures considered here originated in a diagenetic pyrite sheet which was broken up into individual plates during later deformation. Quartz fibres grew syntectonically between the spreading pyrite plates and their geometry is related to the regional deformation history (Durney 1971, Casey *et al.* 1983). We have measured CL of specimens from two different geological environments. One example (Fig. 8) is a chocolate tablet from Parys Mountain, Anglesey, U.K. The deformation history, which can be deduced from the fibre geometry at this locality, has been discussed by Casey *et al.* (1983). The strain recorded in this structure parallel to the finite XY-plane amounts to $1 + e_1 = 1.63$, and $1 + e_2 = 1.17$ (Casey *et al.* 1983, p. 218). The second example (D 358, Figs. 2 and 9) also contains quartz fibre veins and comes from the uppermost Helvetic nappe, the Wildhorn nappe. This specimen is representative of a state of low finite strain of the surrounding limestone, with $1 + e_1 = 1.24$ and $1 + e_2 = 0.99$. The growth sense of the fibres is in both cases antitaxial.

Six spectra were recorded from the Anglesey specimen and all have an overall similar shape, showing a broad red band luminescence. Figure 10(a) shows a spectrum of the oldest part of the fibres, in the centre of the vein, and Fig. 10(b) a spectrum from the youngest fibres, close to the pyrite. The main difference is that the spectrum from the youngest fibres shows a shift of the main peak towards red, in relation to a relatively weaker blue band component. This is also seen in the intensity ratios given in Table 1.

The two spectra recorded from the short fibres of the Helvetic chocolate tablet structure, D 358, have a blue band component roughly similar to the older pressure shadow fibres of D 121 (Fig. 4a), and to the older part of the Anglesey fibres (Fig. 10a). Figure 11 shows one of the D 358 spectra.

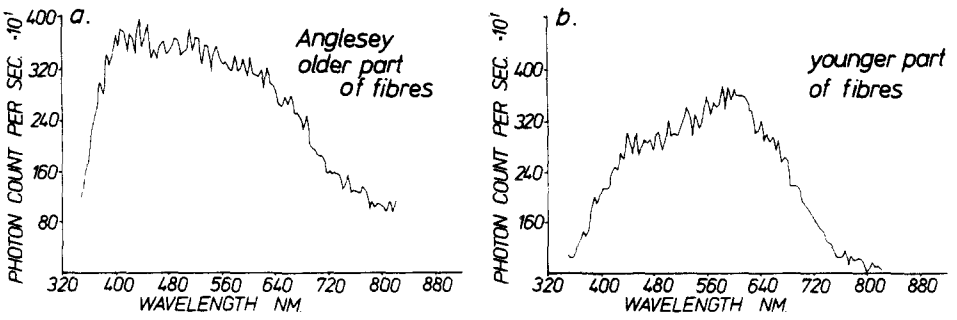

Fig. 10. Spectra from the Anglesey specimen. (a) Spectrum from the older part of the fibres. (b) Spectrum from the younger part of the fibres.

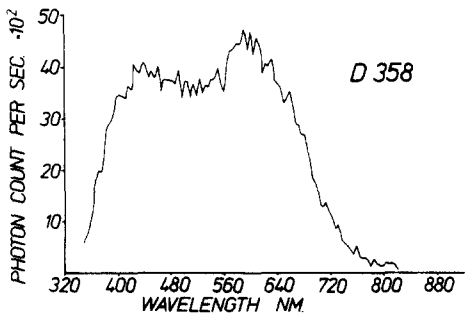

Fig. 11. Spectrum from the Helvetic chocolate tablet structure, D 358.

It is instructive to examine the relative red band intensities recorded from the Helvetic specimens D 121 and D 358 (Figs. 4 and 11) in more detail. Whereas the red peak in the D 358 spectra is only slightly better defined than the blue peak, there is a more pronounced difference in the definition of the two peaks in the spectra of the older fibres of D 121, and this difference becomes even greater in the spectra of the younger fibres. There is a systematic increase in red band intensity and therefore a shift of the main spectral peak towards red from D 358, which comes from the top of the nappe pile, to the older part and finally to the younger part of D 121, which is from the lowermost nappe. We have used illite crystallinity data from shaly horizons close to both specimens to get an estimate of the maximum temperature to which the carbonate units containing the two specimens had been subjected. The Kübler index (Kübler 1968) for specimen D 358 was 8.2, indicating a lower temperature than for specimen D 121 for which an index of 5.0 was determined. The finite deformation in the external part of the Wildhorn nappe is generally low, and Dietrich & Song (1984) have not found any crystallographic preferred orientation in the limestones from that part of the nappe. These observations suggest an essential temperature dependency for the intensity of luminescence of the red band, consistent with the observations of Sprunt *et al.* (1978). These authors observed that undeformed detrital quartz grains "luminesce shades of red and blue", whereas "cathodoluminescence in metamorphosed samples is relatively homogeneous" (Sprunt *et al.* 1978, p. 307).

The presence of a blue spectral component, which widens the spectra of the older fibres of specimen D 121 and of D 358 (Table 1) appears to be independent of temperature. A comparison of the spectrum for the Fernigen sample, D 468 (Fig. 6), with the spectra for D 121 (Figs. 4a & b) leads to the same conclusion. The temperature conditions are assumed to have been similar in both localities, but the relative intensity of the blue peak is different. Its possible dependency on strain rate is discussed in the next example, for which we can assume constancy of this variable.

Tectonic veins

Because of the preponderance of carbonate-rich country rock, fibrous quartz infilling syntectonic veins is relatively rare in the Helvetic nappes. Those fibre veins that do occur often show evidence in thin section for stepwise growth, a process which has been termed "crack–seal" by Ramsay (1980). Crack–seal veins can grow either antitaxially, that is new growth increments get successively added at the vein/wall rock interface, or the already existing fibre vein can grow by different crack–seal events which may not be attributed to a geometrically regular growth sequence (stretched crystal fibres of Durney & Ramsay, 1973). CL has been measured from both types of crack–seal veins.

Specimen D 14a (Figs. 2 and 12) is a vein with fibres at one side which contain regularly spaced bands of inclusions of matrix rock minerals. These inclusion bands indicate antitaxial growth. At a certain point in the development of the vein the rate of crystallization could no longer keep up with the rate of opening, so that the left side of the vein is occupied by blocky crystals, which have partly crystallized out of a fluid phase. We recorded 13 spectra from the fibrous part of the vein, and four spectra from the blocky part. The results for the fibres are similar to those previously described, that is the spectra are generally fairly broad, with a distinguishable blue band which is least pronounced in the youngest part of the fibre (Figs. 13a & b). A spectrum typical of the blocky minerals is shown in Fig. 13(c). It has a blue shoulder, but the relative red band intensity is much higher. Since the crack–seal increments of the fibrous part are of a fairly constant width, we can assume comparable growth conditions during the individual sealing events, and thus *a priori* comparable microstructures in the increments. It seems unlikely that a variation of the strain rate would have influenced the mechanism of growth of the individual increments. The difference between the development of the blue band in Figs. 13(a) and (b) could therefore be a deformation-induced feature. In all three examples where we measured CL parallel to fibres, we found that the blue peak is better developed in the older and therefore more deformed part of the fibres (Figs. 4, 10 and 13).

Specimen 27a (Figs. 2 and 14) is one of the crack–seal veins of Ramsay (1980). It comes from the Helvetic Tertiary ironstone, and contains clastic quartz which is derived from the basement. The veinlets cut through these quartz grains and the crystallographic orientation of the Alpine vein quartz is controlled by the pre-Alpine quartz clasts. Each veinlet corresponds to an individual crack–seal event, but these have not developed with any evident geometrically systematic sense of growth. Figure 14 is an optical CL micrograph at 5 kV taken by U. Zinkernagel. The quartz clasts appear bright violet under optical CL, and slices of the clasts between the veinlets can be identified because they show similar colours to the parent grain. The quartz in the veinlets appears blue. Figure 15(a) is representative of the seven spectra recorded from clastic quartz, and Fig. 15(b) representative of 24 spectra recorded from vein quartz; these spectra being measured at 30 kV. The spectrum for clastic quartz has a characteristic single blue peak, whereas that for the vein quartz shows a broad double

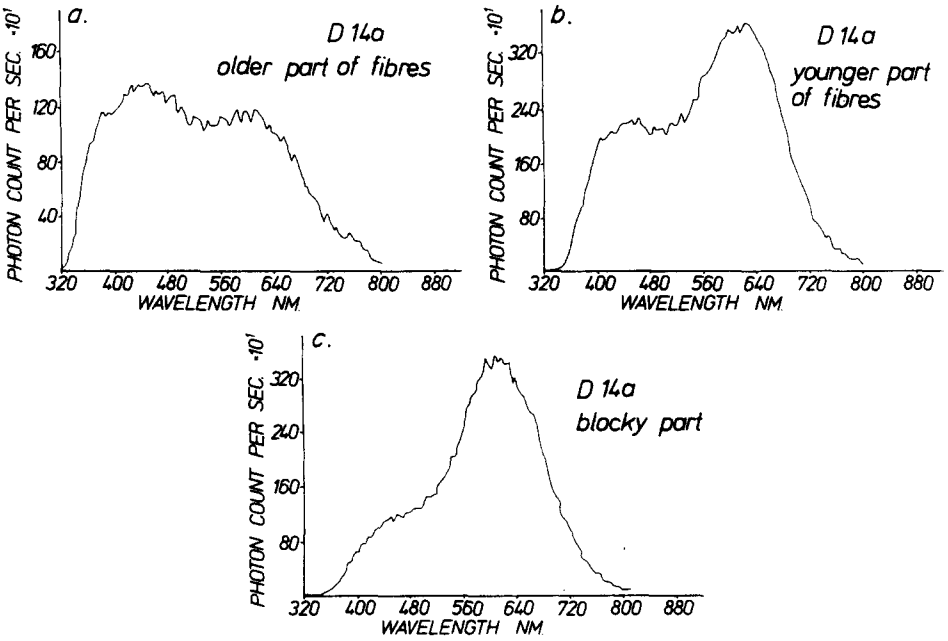

Fig. 13. Spectra from the vein D 14a. (a) From older part of the fibres. (b) From younger part of the fibres. (c) From blocky crystals.

peak. This clearly reflects a difference between the clasts and the veins in the degree of order in the quartz lattice structure.

COMPARISON OF THE RESULTS WITH CATHODOLUMINESCENCE OBSERVATIONS BY OPTICAL MICROSCOPY

To what extent are the differences among the measured spectra discussed above detectable under an optical microscope with a CL attachment? A. Matter and K. Ramseier (Geologisches Institut, Universität Bern) and U. Zinkernagel (Institut für Geologie, Ruhr-Universität Bochum) kindly made available to us their optical CL devices. Operating voltages were 30 kV at Bern, and 5 kV at Bochum. At higher voltages and current flux it was found that lattice damage soon occurred, and this damage altered the CL colour. The luminescence of the fibres investigated was very weak, of a dull brown colour, and partially dominated by the brighter luminescence of the carbonate matrix. No clear difference in CL colour could be observed between older and younger parts of fibres, or between fibres from more strongly or more weakly deformed regions. Only in the case of specimen 27a could clastic quartz and vein quartz be distinguished (Fig. 14). Optical CL microscopy also indicated uniformity of luminescence colours between different fibres in the same structure. This uniformity occurs despite an evident orientation anisotropy of the fibres, that is adjacent fibres in veins and pressure shadows show different c-axis orientations. CL thus indicated no variation of the emitted light intensity or colour with variable crystallographic orientations.

A sequence of spectra at different operating voltages was determined with SEM CL. Figures 16(a)–(e) show five spectra from the older part of the fibres in the pressure shadow of specimen D 121, and Figs. 16(f)–(j) show five spectra from the younger part. As operating voltages are lowered the spectra show a systematic decrease in overall intensities, with the red and the blue peaks disappearing in a general low intensity broad band (Figs. 16a & f). However the spectrum from the older fibres at 10 kV (Fig. 16b) is already slightly wider than the corresponding spectrum from the younger fibres (Fig. 16g). At 20 kV the blue band intensity of the

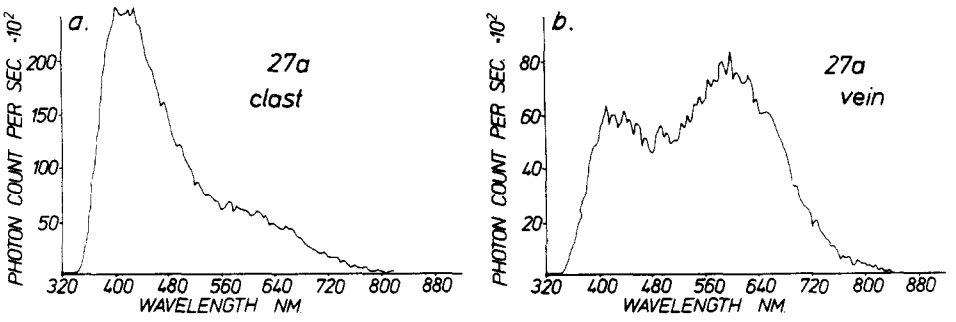

Fig. 15. Spectra from vein 27a. (a) From clastic quartz. (b) From vein quartz.

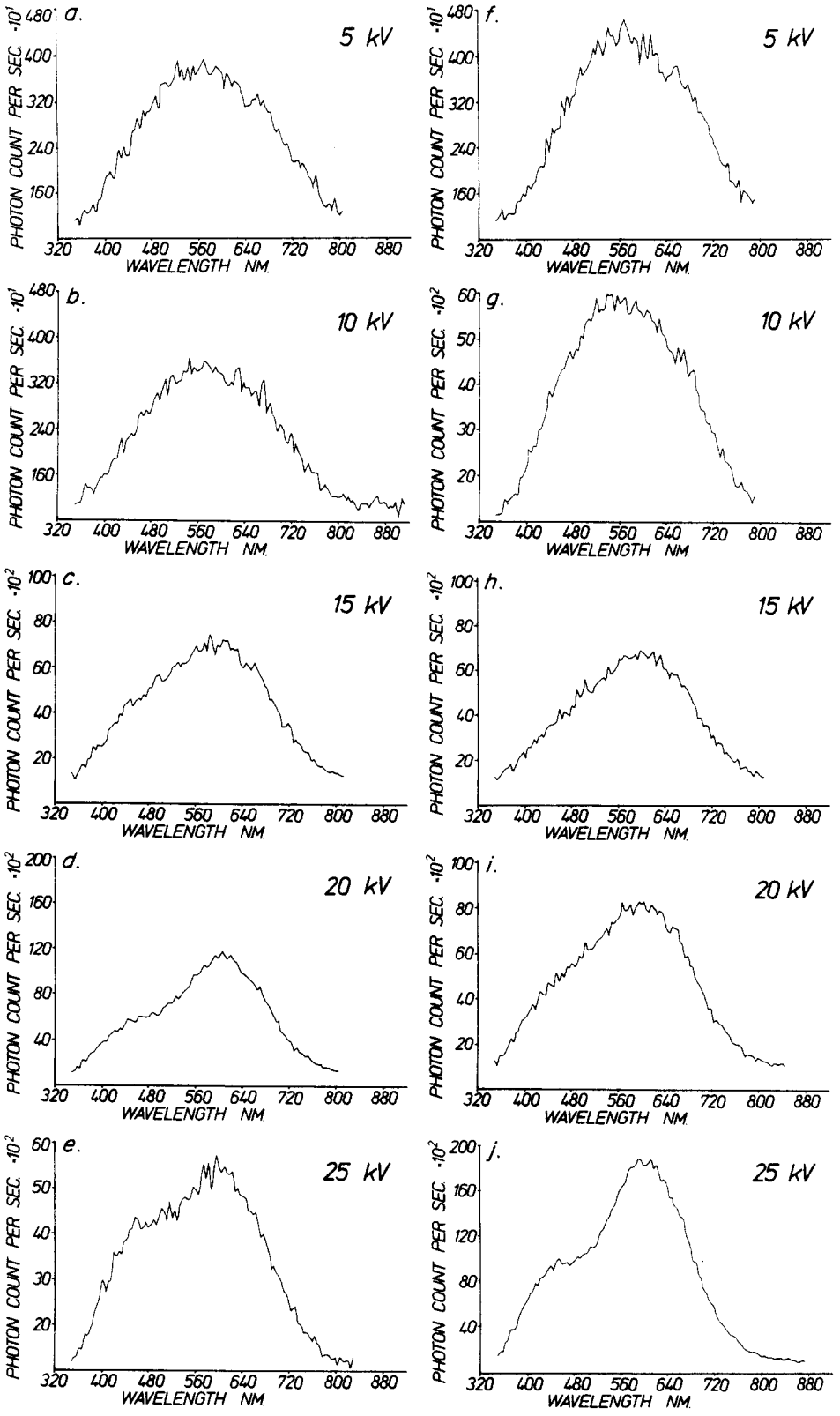

Fig. 16. Spectra from pressure shadow D 121. (a)–(e) From older part of the fibres, at 5, 10, 15, 20 and 25 kV. (f)–(j) from younger part of the fibres, at 5, 10, 15, 20 and 25 kV.

spectrum is visibly stronger in the older fibres (Fig. 16d) than in the younger fibres (Fig. 16i). The subtle distinctions we have been able to observe in the form of the CL spectra of low grade quartz are therefore dependent on the availability of an SEM operated at high voltage, and on the possibility of a spot analysis which enables minerals with weak light emissions to be studied in the presence of neighbouring minerals with high emissivity.

CONCLUSIONS

Measurements of cathodoluminescence of syntec-

tonically grown quartz fibres in veins and pressure shadows from carbonate units with different deformational histories have produced interesting results. We have found characteristic double-peak spectra for all the low-grade quartz fibres analysed. Systematic variations in the form of the measured spectra could be observed. A relatively higher red band intensity could be related to a higher temperature during fibre growth, that is during the deformation of the rock unit containing the fibres. A relatively higher blue band intensity is apparently not related to temperature or strain rate during fibre growth. Relatively strong blue bands are restricted to older parts of fibres and have therefore to be related to lattice modifications induced by continuing deformation of the earlier formed fibres.

Distinctive variations of the spectra for low-grade quartz could only be observed with the SEM at high operating voltage. At lower voltages, as usually employed in optical CL microscopy, only broad, undifferentiated spectra of low intensity could be measured. We add here a note of caution: because of this variability in response of materials to electron beam bombardment great care is necessary in comparing results of different workers.

Acknowledgements—We thank A. Matter, K. Ramseier and U. Zinkernagel for having made available their optical CL devices, and for interesting discussions. We acknowledge constructive reviews of this article by Rob Knipe, John Ramsay and Karl Ramseier, and the referees of the *Journal of Structural Geology*. Discussions on specific points with Martin Casey and John Ridley were helpful.

DD was supported by Schweizerischer Nationalfonds, Project No. 5.521.330.880/5.

REFERENCES

Casey, M., Dietrich, D. & Ramsay, J. G. 1983. Methods for determining deformation history for chocolate tablet boudinage with fibrous crystals. *Tectonophysics* **92**, 211–239.

Dietrich, D. & Song, H. 1984. Calcite fabrics in a natural shear environment, the Helvetic nappes of Western Switzerland. *J. Struct. Geol.* **6**, 19–32.

Durney, D. W. 1971. Deformation history of the Western Helvetic nappes, Valais, Switzerland. Unpublished Ph.D. thesis, University of London.

Durney, D. W. & Ramsay, J. G. 1973. Incremental strains measured by syntectonic crystal growth. In: *Gravity and Tectonics* (edited by De Jong, K. & Scholten, R.). Wiley, New York, 67–96.

Frey, M., Teichmüller, M., Teichmüller, R., Mullis, J., Künzi, B., Breitschmid, A., Gruner, U. & Schwizer, B. 1980. Very low-grade metamorphism in external parts of the central Alps: illite crystallinity, coal rank and fluid inclusion data. *Eclog. geol. Helv.* **73**, 173–203.

Grant, P. R. 1978. The role of the scanning electron microscope in cathodoluminescence petrology. In: *Scanning Electron Microscopy in the Study of Sediments* (edited by Whalley, W. B.). Geo Abstracts, Norwich, U.K.

Grant, P. R. & White, S. H. 1978. Cathodoluminescence and microstructure of quartz overgrowths on quartz. *Scanning Electron Microsc.* **1**, 789–793.

Hanusiak, W. M. & White, E. W. 1975. SEM cathodoluminescence for characterisation of damaged and undamaged α-quartz in respirable dusts. *Proc. 8th Annual SEM Symposium*, IITRI, Chicago, 125–131.

Holt, D. B. & Odgen, R. 1976. Observation of dislocations in a silicon phototransitor by Scanning Electron Microscopy using the barrier electron voltaic effect. *Solid State Electronics* **19**, 37–40.

Kübler, B. 1968. Evaluation quantitative du métamorphisme par cristallinité de l'illite. *Bull. Centre Rech. Pau*, SNPA, **2**, 385–397.

Muir, M. D. & Grant, P. R. 1974. Cathodoluminescence. In: *Quantitative Scanning Electron Microscopy* (edited by Holt, D. B., Muir, M. D., Grant, P. R. & Boswarva, I. M.), Chapter 9, Academic Press, London.

Ramsay, J. G. 1980. The crack–seal mechanism of rock deformation. *Nature, Lond.* **284**, 135–139.

Schmid, S. M. 1982. Laboratory experiments on rheology and deformation mechanisms in calcite rocks and their application to studies in the field. *Mitteilungen aus dem Geologischen Institut ETH und Universität Zürich*, N.F. 241.

Sibley, D. F. 1975. *Extension Microfractures in the Tuscarora Orthoquartzite, Evidence from Luminescence Petrography*. Nuclide Corporation, Acton, MA, U.S.A.

Sommer, S. E. 1972. Cathodoluminescence of carbonates—1. Characterization of cathodoluminescence from carbonate solid solutions. *Chem. Geol.* **9**, 257–273.

Sprunt, E. S. 1981. Causes of quartz cathodoluminescence colours. *Scanning Electron Microsc.* **1**, 525–535.

Sprunt, E. S., Dengler, L. A. & Sloan, D. 1978. Effects of metamorphism on quartz cathodoluminescence. *Geology* **6**, 305–308.

Steyn, J. B., Giles, P. & Holt, D. B. 1976. An efficient spectroscopic detection system for cathodoluminescence mode scanning electron microscopy (SEM). *J. Microscopy* **107**, 107–128.

Zinkernagel, U. 1978. Cathodoluminescence of quartz and its application to sandstone petrology. *Contr. Sediment.* **8**, 1–69.